Journal of Computational Physics **164,** 22–47 (2000)
doi:10.1006/jcph.2000.6585, available online at http://www.idealibrary.com on IDEAL®

Estimation of Local Modeling Error and Goal-Oriented Adaptive Modeling of Heterogeneous Materials

I. Error Estimates and Adaptive Algorithms

J. Tinsley Oden and Kumar S. Vemaganti

Texas Institute for Computational and Applied Mathematics, The University of Texas at Austin, Austin, Texas
E-mail: oden@ticam.utexas.edu, kumar@ticam.utexas.edu

Received February 10, 2000; revised July 10, 2000

DEDICATED TO PROFESSOR ROGER TEMAM ON THE OCCASION OF HIS 60TH BIRTHDAY

A theory of a posteriori estimation of modeling errors in local quantities of interest in the analysis of heterogeneous elastic solids is presented. These quantities may, for example, represent averaged stresses on the surface of inclusions or mollifications of pointwise stresses or displacements or, in general, local features of the "fine-scale" solution characterized by continuous linear functionals. These estimators are used to construct goal-oriented adaptive procedures in which models of the microstructure are adapted to deliver local features to a preset level of accuracy. Algorithms for implementing these procedures are discussed and preliminary numerical results are given. The analysis is restricted to linear, static, heterogeneous, elastic materials.

Key Words: heterogeneous materials; hierarchical modeling; modeling error; local error; estimates.

CONTENTS

0021-9991/00 $35.00

1. INTRODUCTION

The idea of automatically adapting characteristics of mathematical and computational models of heterogeneous media to obtain results of a specified level of accuracy was advanced in recent work on *hierarchical modeling* [8, 12]. In these papers, a posteriori bounds on the error in solutions to elastostatics problems induced by replacing fine-scale micromechanical properties by coarser scale or effective properties were derived in global energy norms. These error estimates were then used as a basis for an *adaptive modeling process* in which only enough fine-scale information sufficient to deliver results of a preset accuracy, measured in energy norms, is used to characterize the model. The resulting adaptive process can lead to significant computational savings, making possible the analysis of micromechanical effects in some cases that are intractable by traditional approaches. Preliminary results on extensions of these adaptive approaches to a class of models depicting material damage were discussed in [7].

It is clear that adaptive procedures based on energy-norm estimates may be insensitive to very localized features of the fine-scale solution. Modeling error in characterizing average stresses on interfaces or on surfaces of inclusions, for example, may not be detected by energy-norm estimates unless virtually all of the fine-scale information is used in defining the computational/mathematical model. To efficiently control the accuracy of models of such local features, local estimates of modeling error are required.

In the present paper, we extend the theory of a posteriori modeling error estimation for heterogeneous materials to "quantities of interest," by which we mean local features of the response. In our theory, these quantities of interest could represent, for example, average stresses on material interfaces, boundary displacements, or mollified pointwise displacements, strains, or stresses. We remark that many candidates for local quantities of interest are, in fact, quantities that one actually measures in assessing mechanical response—strains at points as averaged relative displacements over a strain gauge, local stresses as forces distributed over interior surfaces, etc. More is said about such quantities of interest in Sections 3 and 5. Mathematically, a quantity of interest is any feature of the fine-scale solution that can be characterized as a continuous linear functional on the space of functions to which the fine-scale solution belongs. We establish computable upper and lower bounds and sharp estimates of the errors in such quantities.

With local error estimates available, we develop *goal-oriented adaptive procedures*, in which the model is automatically adapted to deliver local quantities of interest to within a preset level of accuracy. These procedures are reminiscent of recently developed goal-oriented adaptive procedures for controlling numerical approximation error in linear functionals [9]. In the present investigation, we present an adaptive procedure that, in principle, utilizes only information on fine-scale structures in a neighborhood of the local feature of interest sufficient to produce results of preset level of accuracy; information outside this neighborhood need only reflect the response of models defined using effective, homogenized properties of the material.

Some basic features and assumptions underlying the approaches described here should be noted:

1. By an exact, fine-scale model, problem, or solution, we mean the exact solution $\mathbf{u}$ to a weak boundary value problem in elastostatics in which the elastic coefficients are characterized by a possibly rapidly varying elasticity tensor $\mathbf{E} = \mathbf{E}(\mathbf{x})$ which is known a priori. The modeling error $\mathbf{e}$ is the function defined as the difference between $\mathbf{u}$ and any coarse-scale

solution $\tilde{\mathbf{u}}$ to an elastostatics problem defined on the same domain, subjected to the same external forces as the fine-scale problem, but with a different elasticity tensor $\tilde{\mathbf{E}}$ as coefficients in the problem: $\mathbf{e} = \mathbf{u} - \tilde{\mathbf{u}}$. The function $\tilde{\mathbf{u}}$, for example, could be the "homogenized solution" $\mathbf{u}^0$, the solution of the problem in which effective properties, characterized by a constant or piecewise constant "homogenized" elasticity tensor $\mathbf{E}^0$, are used.

2. In applications of our theory and algorithms, the coarse-scale solutions are generally computed using various numerical methods, such as finite elements. But estimation of numerical error is not considered in this paper; the techniques developed in [1, 9] can be used to control approximation error. Our concern here is *modeling error* in the sense discussed above, and this error can have properties and behavior quite different from those of numerical approximation error.

3. In theory, the tensor field $\mathbf{E}(\mathbf{x})$ defines at almost every point $\mathbf{x}$ in the body an array $(E_{ijkl}(\mathbf{x}))$ with the standard ellipticity and symmetry properties. In our applications, $\mathbf{E}$ is generally piecewise constant, representing a so-called n-phase material with n isotropic phases, $n > 1$. For a large class of such materials, it is possible to represent the function $\mathbf{E}$ characterizing the fine-scale microstructure with sufficient accuracy using actual X-ray computed tomography (CT) imaging procedures with the overall model adaptivity package to characterize $\mathbf{E}$. The important details of this feature of adaptive modeling are the subject of a companion paper [11]. As will be seen later in this paper, only CT data sufficient to define $\mathbf{E} = \mathbf{E}(\mathbf{x})$ in local neighborhoods of features of interest are needed; the enormous data storage requirements of a global characterization of $\mathbf{E}$ called for in earlier global approaches are, in general, not needed in the goal-oriented adaptivity approaches advocated here.

4. It is important to emphasize that our goal is *not* to estimate effective properties of heterogeneous materials. Indeed, the familiar process of homogenization of fine-scale features of the coefficients is here only a mathematical artifact embedded in a broader computational strategy. Our error estimates and adaptive procedures apply to modeling errors in any kinematically admissible function, independent of the coefficients, so long as the underlying problem is well posed. Nevertheless, the choice of approximations or regularizations of $\mathbf{E}$ will obviously affect modeling error and rates of convergence of the adaptive process to models delivering results with the target accuracies.

5. Extensions of our adaptive procedures to nonlinear problems are possible, although such extensions are not considered here. These extensions could involve incorporating the goal-oriented adaptive process as an inner loop in a broader iterative process, assuming that the regularized problem remains well defined. In effect, such extensions amount to redefining the level of sophistication of the model used as a datum for error estimation.

In the next section, we describe the model class of problems and lay down notations and preliminaries. We then establish a series of results on local estimates of errors in quantities of interest, including upper and lower bounds on errors. This is followed by the description of a goal-oriented adaptive modeling algorithm. An analysis of the algorithm and results of preliminary numerical implementations are then presented. The detailed description of a computational environment designed to automate such procedures and the interface with imaging and visualization modules is the subject of forthcoming work [11].

2. NOTATIONS AND PRELIMINARIES

We consider an open bounded $\Omega \subset \mathbb{R}^N$, $N = 1, 2$, or 3, with boundary $\partial\Omega$. In general, Ω can be multiconnected and very irregular, but for present purposes, it suffices to take Ω

to be Lipschitz with piecewise smooth boundaries. We denote by $H^m(\Omega)$, $m \geq 0$, the space of functions with distributional derivatives of order $\leq m$ in $L^2(\Omega)$ and we use the notation $\mathbf{H}^m(\Omega) \stackrel{\text{def}}{=} (H^m(\Omega))^N$ and $\mathbf{L}^2(\Omega) \stackrel{\text{def}}{=} (L^2(\Omega))^N$.

The closure of Ω is the region occupied by a linearly elastic material body in static equilibrium under the action of body forces $\mathbf{f} \in \mathbf{L}^2(\Omega)$ and surface tractions $\mathbf{t} \in \mathbf{L}^2(\Gamma_t)$, with $\Gamma_t \subset \partial\Omega$. The displacements $\mathbf{u}$ of the body are prescribed as zero on $\Gamma_u = \partial\Omega \backslash \Gamma_t$. The space of admissible functions $\mathbf{V}(\Omega)$ is therefore defined as

$$\mathbf{V}(\Omega) \stackrel{\text{def}}{=} \{\mathbf{v} : \mathbf{v} \in \mathbf{H}^1(\Omega), \mathbf{v}|_{\Gamma_u} = \mathbf{0}\}, \tag{1}$$

the boundary values being understood in the sense of traces of H^1 functions. In general, we will assume that meas $\Gamma_u > 0$; otherwise, our development is only altered by replacing $\mathbf{V}(\Omega)$ with $\mathbf{V}(\Omega)\backslash\mathbf{R}(\Omega)$, $\mathbf{R}(\Omega)$ being the linear space of infinitesimal rigid motions of the body.

The total potential energy of the body is characterized by the functional

$$\begin{aligned} \mathcal{J} &: \mathbf{V}(\Omega) \to \mathbb{R} \\ \mathcal{J}(\mathbf{v}) &\stackrel{\text{def}}{=} \frac{1}{2}\mathcal{B}(\mathbf{v}, \mathbf{v}) - \mathcal{F}(\mathbf{v}), \end{aligned} \tag{2}$$

where $\mathcal{B}(\cdot, \cdot)$ is the symmetric, positive-definite, bilinear form,

$$\begin{aligned} \mathcal{B} &: \mathbf{V}(\Omega) \times \mathbf{V}(\Omega) \to \mathbb{R} \\ \mathcal{B}(\mathbf{u}, \mathbf{v}) &\stackrel{\text{def}}{=} \int_\Omega \boldsymbol{\nabla}\mathbf{v} : \mathbf{E}\boldsymbol{\nabla}\mathbf{u}\, d\mathbf{x}, \end{aligned} \tag{3}$$

and $\mathcal{F}(\cdot)$ is the linear functional,

$$\begin{aligned} \mathcal{F} &: \mathbf{V}(\Omega) \to \mathbb{R} \\ \mathcal{F}(\mathbf{v}) &\stackrel{\text{def}}{=} \int_\Omega \mathbf{f} \cdot \mathbf{v}\, d\mathbf{x} + \int_{\Gamma_t} \mathbf{t} \cdot \mathbf{v}\, d\mathbf{s}. \end{aligned} \tag{4}$$

It is also convenient to introduce the weighted inner product $((\cdot, \cdot))_E$ on $(L^2(\Omega))^{N^2} \times (L^2(\Omega))^{N^2}$ defined by

$$((\mathbf{A}, \mathbf{B}))_E \stackrel{\text{def}}{=} \int_\Omega \mathbf{A} : \mathbf{E}\mathbf{B}\, d\mathbf{x} \tag{5}$$

for tensor fields $\mathbf{A}$, $\mathbf{B}$. Then, $\mathcal{B}(\mathbf{u}, \mathbf{v}) = ((\boldsymbol{\nabla}\mathbf{v}, \boldsymbol{\nabla}\mathbf{u}))_E$ and

$$((\boldsymbol{\nabla}\mathbf{v}, \boldsymbol{\nabla}\mathbf{v}))_E = \mathcal{B}(\mathbf{v}, \mathbf{v}) = \|\mathbf{v}\|^2_{E(\Omega)}, \tag{6}$$

where $\|\cdot\|_{E_{(\Omega)}}$ is the *energy norm* of $\mathbf{v}$.

In (3), $\mathbf{E} \in (L^\infty(\Omega))^{N^2 \times N^2}$ is the uniformly elliptic tensor of elasticities which satisfies the standard symmetry conditions: $E_{ijkl}(\mathbf{x}) = E_{jikl}(\mathbf{x}) = E_{ijlk}(\mathbf{x}) = E_{klij}(\mathbf{x})$, for a.e. $\mathbf{x}$ in Ω, $1 \leq i, j, k, l \leq N$. The notation (:) denotes contraction of second-order tensors ($\boldsymbol{\nabla}\mathbf{v} : \mathbf{E}\boldsymbol{\nabla}\mathbf{u} = v_{i,j} E_{ijkl} u_{k,l}$, summing on i, j, k, l, $v_{i,j} = \partial v_i / \partial x_j$; $u_{k,l} = \partial u_k / \partial x_l$). There, also, $d\mathbf{x} = dx_1\, dx_2 \cdots dx_N$ is the volume measure and $d\mathbf{s}$ the surface element.

The material characterized by $\mathbf{E}$ is assumed to have a complex, not necessarily periodic microstructure so that $\mathbf{E}$ is a highly oscillatory function of position $\mathbf{x}$ over Ω.

2.1. *The Fine-Scale Problem*

Under the stated assumptions, the displacement field $\mathbf{u} \in \mathbf{V}(\Omega)$ that exists when the body is in static equilibrium under the action of external forces $(\mathbf{f}, \mathbf{t})$ is the unique admissible displacement that minimizes $\mathcal{J}$ over $\mathbf{V}(\Omega)$ and is the unique solution to the following weak boundary value problem:

$$\begin{gathered} \text{Find } \mathbf{u} \in \mathbf{V}(\Omega) \text{ such that} \\ \mathcal{B}(\mathbf{u}, \mathbf{v}) = \mathcal{F}(\mathbf{v}) \quad \forall\, \mathbf{v} \in \mathbf{V}(\Omega). \end{gathered} \tag{7}$$

We shall refer to (7) as the *fine-scale problem* since it involves all the fine-scale features of the material, and to its solution $\mathbf{u}$ as the *fine-scale solution*. In the sense of distributions, (7) is equivalent to the elliptic system,

$$\begin{aligned} -\boldsymbol{\nabla} \cdot \boldsymbol{\sigma} &= \mathbf{f} \\ \boldsymbol{\sigma} &= \mathbf{E}\varepsilon \\ 2\varepsilon &= \boldsymbol{\nabla}\mathbf{u} + \boldsymbol{\nabla}\mathbf{u}^{\mathrm{T}} \\ \mathbf{u} &= \mathbf{0} \text{ on } \Gamma_u \\ \boldsymbol{\sigma} \cdot \mathbf{n} &= \mathbf{t} \text{ on } \Gamma_t, \end{aligned} \tag{8}$$

where $\mathbf{n}$ is the unit outward normal to $\partial\Omega$, and $\boldsymbol{\sigma}$ and ε are the stress and strain tensor fields, respectively.

2.2. *The Regularized Problem*

Various regularizations of problem (9) are obtained by replacing $\mathbf{E}$ with a regularized elasticity tensor. For example, if the microstructure is assumed to be periodic, it is common practice to replace $\mathbf{E}$ with a *homogenized elasticity tensor* $\mathbf{E}^0$, defining *effective properties* of the material, usually a constant tensor. For details on homogenization of periodic composites, see [4, 10]. Another approach used to regularize heterogeneous materials assumes the existence of a representative volume element (RVE); see, for example, [3]. Our approach, however, does not rely on the existence of an RVE for a given heterogeneous material. Without restricting ourselves to a constant function, we assume that the elasticity tensor $\mathbf{E}$ is replaced by a suitable approximation $\mathbf{E}^0$ that satisfies the uniform ellipticity and symmetry conditions. We then can consider the *regularized* or *homogenized problem*,

$$\begin{gathered} \text{Find } \mathbf{u}^0 \in \mathbf{V}(\Omega) \text{ such that} \\ \mathcal{B}^0(\mathbf{u}^0, \mathbf{v}) = \mathcal{F}(\mathbf{v}) \quad \forall \mathbf{v} \in \mathbf{V}(\Omega), \end{gathered} \tag{9}$$

where now

$$\mathcal{B}^0(\mathbf{u}^0, \mathbf{v}) \stackrel{\text{def}}{=} \int_\Omega \boldsymbol{\nabla}\mathbf{v} : \mathbf{E}^0 \boldsymbol{\nabla}\mathbf{u}^0 \, d\mathbf{x}, \tag{10}$$

and $\mathcal{F}(\cdot)$ is again given by (4). The unique solution $\mathbf{u}^0$ to (9) is called the *regularized* or *homogenized solution*.

2.3. *Review of Energy Estimates of the Modeling Error*

The modeling error is defined as the difference between the fine-scale solution and the regularized solution

$$\mathbf{e}^0 \stackrel{\text{def}}{=} \mathbf{u} - \mathbf{u}^0. \tag{11}$$

We now review two results of the estimation of this error in the energy norm. For this purpose, we define

$$\mathcal{I}_0 = (\mathbf{I} - \mathbf{E}^{-1}\mathbf{E}^0), \tag{12}$$

where $\mathbf{I}$ is the identity tensor. Next, for $\mathbf{g} \in \mathbf{V}$, we define the associated linear *residual functional* $\mathcal{R}_\mathbf{g} : \mathbf{V}(\Omega) \to \mathbb{R}$,

$$\mathcal{R}_\mathbf{g}(\mathbf{v}) = -\int_\Omega \boldsymbol{\nabla}\mathbf{v} : \mathbf{E}\mathcal{I}_0\boldsymbol{\nabla}\mathbf{g}\, d\mathbf{x}, \quad \mathbf{v} \in \mathbf{V}(\Omega). \tag{13}$$

THEOREM 2.1. *Let* $\mathbf{u}$ *and* $\mathbf{u}^0$ *be the solutions to problems* (7) *and* (9)*, respectively. Then the following holds,*

$$\zeta_{\text{low}} \le \|\mathbf{e}^0\|_{E(\Omega)} = \|\mathbf{u} - \mathbf{u}^0\|_{E(\Omega)} \le \zeta_{\text{upp}}, \tag{14}$$

where

$$\zeta_{\text{low}} \stackrel{\text{def}}{=} \frac{|\mathcal{R}_{\mathbf{u}^0}(\mathbf{u}^0)|}{\|\mathbf{u}^0\|_{\text{E}(\Omega)}}, \quad \zeta_{\text{upp}} \stackrel{\text{def}}{=} ((\mathcal{I}_0\boldsymbol{\nabla}\mathbf{u}^0, \mathcal{I}_0\boldsymbol{\nabla}\mathbf{u}^0))_E^{1/2}. \tag{15}$$

For proofs, see [12] and [6]. Both assertions follow from the fact that the modeling error $\mathbf{e}^0$ is governed by

$$\mathcal{B}(\mathbf{e}^0, \mathbf{v}) = \mathcal{R}_{\mathbf{u}^0}(\mathbf{v}), \quad \forall \mathbf{v} \in \mathbf{V}(\Omega). \tag{16}$$

Using the above result, it is possible to estimate the energy norm of the difference between the fine-scale solution $\mathbf{u}$ and any admissible function $\mathbf{z} \in \mathbf{V}(\Omega)$.

COROLLARY 2.1. *Let* $\mathbf{u}$ *and* $\mathbf{u}^0$ *be the solutions to problems* (7) *and* (9)*, respectively, and let* $\mathbf{z} \in \mathbf{V}(\Omega)\backslash\{\mathbf{0}\}$*. Then,*

$$\zeta^z_{\text{low}} \le \|\mathbf{u} - \mathbf{z}\|_{E(\Omega)} \le \zeta^z_{\text{upp}}, \tag{17}$$

where

$$\zeta^z_{\text{low}} \stackrel{\text{def}}{=} \frac{|\mathcal{F}(\mathbf{z}) - \mathcal{B}(\mathbf{z}, \mathbf{z})|}{\|\mathbf{z}\|_{E(\Omega)}}, \quad \zeta^z_{\text{upp}} \stackrel{\text{def}}{=} \sqrt{2(\mathcal{J}(\mathbf{z}) - \mathcal{J}(\mathbf{u}^0)) + \zeta^2_{\text{upp}}}, \tag{18}$$

with $\mathcal{J}$ *as defined in* (2).

Proof. The proof for the assertion $\|\mathbf{u}-\mathbf{z}\|_{E(\Omega)} \leq \zeta^z_{\text{upp}}$ can be found in [8]. For the lower bound, we have

$$\mathcal{B}(\mathbf{u}-\mathbf{z},\mathbf{v}) = \mathcal{F}(\mathbf{v}) - \mathcal{B}(\mathbf{z},\mathbf{v}) \quad \forall\, \mathbf{v} \in \mathbf{V}(\Omega). \tag{19}$$

Then, it is straightforward to show that

$$\|\mathbf{u}-\mathbf{z}\|_{E(\Omega)} = \sup_{\mathbf{v}\in\mathbf{V}(\Omega)\setminus\{\mathbf{0}\}} \frac{|\mathcal{F}(\mathbf{v}) - \mathcal{B}(\mathbf{z},\mathbf{v})|}{\|\mathbf{v}\|_{E(\Omega)}}, \tag{20}$$

and by picking $\mathbf{v} = \mathbf{z}$, we obtain

$$\|\mathbf{u}-\mathbf{z}\|_{E(\Omega)} \geq \frac{|\mathcal{F}(\mathbf{z}) - \mathcal{B}(\mathbf{z},\mathbf{z})|}{\|\mathbf{z}\|_{E(\Omega)}}, \tag{21}$$

which concludes the proof. ■

3. MODELING ERROR IN LOCAL QUANTITIES OF INTEREST

As mentioned in the Introduction, global estimates of modeling error, such as the energy estimate presented in Theorem 2.1, can be insensitive to local quantities of interest such as interfacial stresses. To address this problem, we now present a theory for the estimation of modeling error in quantities of interest that can be characterized as continuous linear functionals on the space of admissible functions $\mathbf{V}(\Omega)$. This theory represents a significant departure from more traditional theories of error estimation in that it allows the estimation of modeling error in virtually any quantity of interest to the analyst, such as (mollified) pointwise values of stresses and displacements, boundary displacements, and averaged stresses. Concrete examples of such quantities of interest will be given in the section on numerical experiments.

The goal in this section is to obtain bounds on the quantity $L(\mathbf{u}) - L(\mathbf{u}^0) = L(\mathbf{e}^0)$, where $L \in \mathbf{V}'(\Omega)$ is a continuous linear functional. We first present a result on obtaining upper and lower bounds on $L(\mathbf{e}^0)$. Next, we show how this theory can be extended to obtain bounds on the error in *arbitrary admissible* functions $\mathbf{z} \in \mathbf{V}(\Omega)$, i.e., bounds on the quantity $L(\mathbf{u}) - L(\mathbf{z}) = L(\mathbf{u}-\mathbf{z})$, where $\mathbf{z}$ is not necessarily the solution to an elastostatics problem posed on the domain Ω. The motivation behind this is that the modeling error in local quantities of interest can often be reduced by adding perturbations to the regularized solution such that the sum is still an admissible function.

Some comments on why "quantities of interest" are characterized as "continuous linear functions" are appropriate. It is understood that important local features of the micromechanical response are obliterated by homogenization but may be the precise quantities of interest in determining the performance of the material—stresses at material interfaces, relative displacements of inclusions, etc. As will be demonstrated in the next section, the extraction of errors in local features of the response is accomplished by setting up an auxiliary (adjoint) problem for an influence function $\mathbf{w}$ in which the data in the problem (the "right-hand side") are a customized functional characterizing the particular feature of interest. The characterizing functional L must be linear and continuous, or else the auxiliary problem could be meaningless. For example, it would be inappropriate to identify a stress or displacement at a point $\mathbf{x}$ in Ω as a quantity of interest as the "stress could be infinite" and

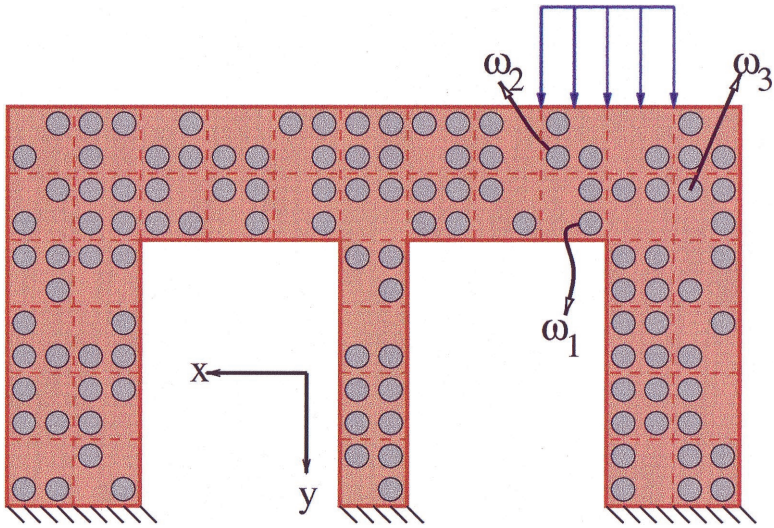

FIG. 1. Schematic of the composite body considered. Dashed lines indicate the partitioning of the domain into cells.

point displacements are underfined in $\mathbf{V}(\Omega)$. Instead, we construct averaged or mollified functions so that the influence function that corresponds to the particular feature of interest is a well-defined admissible function in $\mathbf{V}(\Omega)$. Thus, for example, L could represent average stress components over a small surface area. We give more examples later in Section 5.

3.1. *Upper and Lower Bounds on Modeling Errors in Local Quantities of Interest*

Let L be a continuous linear functional on $\mathbf{V}(\Omega)$, $L \in \mathbf{V}'(\Omega)$. As a first step, we first pose the following global *adjoint fine-scale problem*:

$$\begin{gathered}\text{Find } \mathbf{w} \in \mathbf{V}(\Omega) \text{ such that} \\ \mathcal{B}(\mathbf{v}, \mathbf{w}) = L(\mathbf{v}) \quad \forall\, \mathbf{v} \in \mathbf{V}(\Omega).\end{gathered} \tag{22}$$

The solution $\mathbf{w}$ to the adjoint fine-scale problem is referred to as the *fine-scale influence function*. The regularized version of this problem is referred to as the *adjoint regularized*

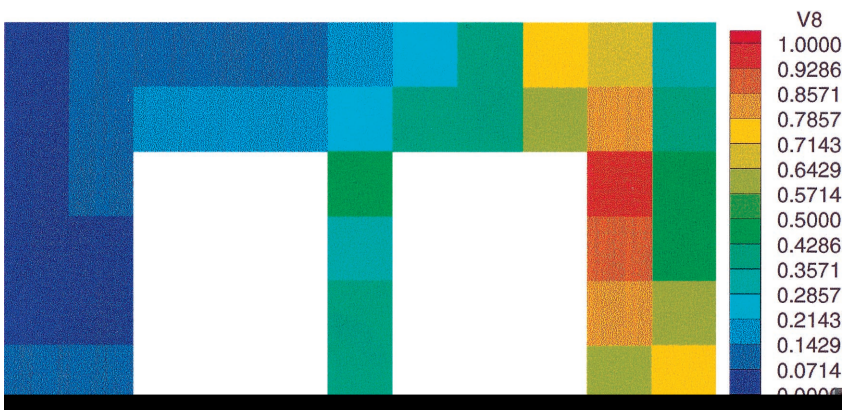

FIG. 2. Distribution of the quantity $\zeta_{k,\text{upp}}$ normalized with respect to the maximum.

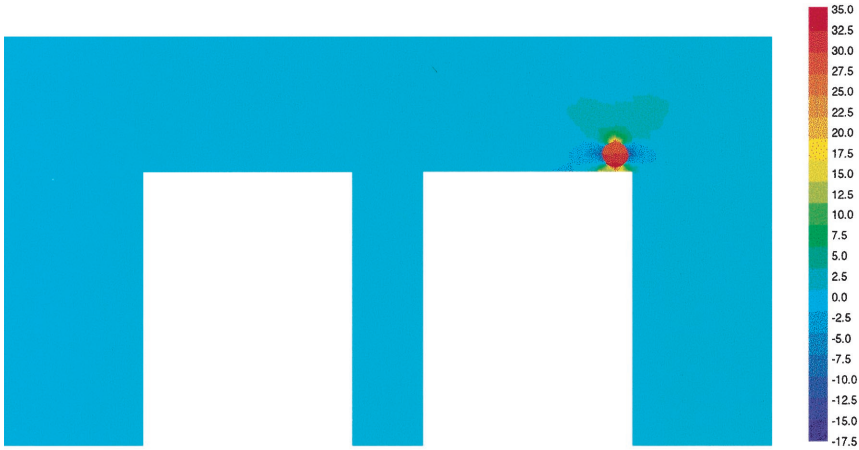

(a)

FIG. 3. Plots of the (a) ε_{11} and (b) ε_{22} components of the strain tensor $\varepsilon(\mathbf{w}^0)$ for the quantity of interest L_1.

problem and reads

$$\begin{gathered}\text{Find } \mathbf{w}^0 \in \mathbf{V}(\Omega) \text{ such that} \\ \mathcal{B}^0(\mathbf{v}, \mathbf{w}^0) = L(\mathbf{v}) \quad \forall\, \mathbf{v} \in \mathbf{V}(\Omega).\end{gathered} \tag{23}$$

The solution to this problem will be referred to as the *regularized influence function*. In what follows, we sometimes refer to the problems (7) and (9) as the *primal fine-scale problem* and *primal regularized problem*, respectively. It is obvious that, under the stated assumptions on $\mathbf{E}$ and $\mathbf{E}^0$, the functions $\mathbf{w}$ and $\mathbf{w}^0$ exist and are uniquely defined.

It immediately follows that the modeling error in the influence function

$$\bar{\mathbf{e}}^0 \stackrel{\text{def}}{=} \mathbf{w} - \mathbf{w}^0 \tag{24}$$

satisfies (recall (16))

$$\mathcal{B}(\mathbf{v}, \bar{\mathbf{e}}^0) = \mathcal{R}_{\mathbf{w}^0}(\mathbf{v}) \quad \forall\, \mathbf{v} \in \mathbf{V}(\Omega). \tag{25}$$

We also note that $\bar{\mathbf{e}}^0$ satisfies the following relationship (analogous to (14)):

$$\bar{\zeta}_{\text{low}} \le \|\bar{\mathbf{e}}^0\|_{E(\Omega)} = \|\mathbf{w} - \mathbf{w}^0\|_{E(\Omega)} \le \bar{\zeta}_{\text{upp}}, \tag{26}$$

where

$$\bar{\zeta}_{\text{low}} \stackrel{\text{def}}{=} \frac{|\mathcal{R}_{\mathbf{w}^0}(\mathbf{w}^0)|}{\|\mathbf{w}^0\|_{E(\Omega)}}; \quad \bar{\zeta}_{\text{upp}} \stackrel{\text{def}}{=} ((\mathcal{I}_0 \boldsymbol{\nabla}\, \mathbf{w}^0, \mathcal{I}_0 \boldsymbol{\nabla} \mathbf{w}^0))_E^{1/2}. \tag{27}$$

We now state the main result of the estimation of modeling error in quantities of interest:

THEOREM 3.1. *Let* $\mathbf{u}^0$ *and* $\mathbf{w}^0$ *be the solutions to problems* (9) *and* (23), *respectively. Then*,

$$\eta_{\text{low}} \le L(\mathbf{e}^0) \le \eta_{\text{upp}}, \tag{28}$$

where

$$\eta_{\text{low}} \stackrel{\text{def}}{=} \frac{1}{4}(\eta_{\text{low}}^+)^2 - \frac{1}{4}(\eta_{\text{upp}}^-)^2 + \mathcal{R}_{\mathbf{u}^0}(\mathbf{w}^0), \tag{29}$$

$$\eta_{\text{upp}} \stackrel{\text{def}}{=} \frac{1}{4}(\eta_{\text{upp}}^+)^2 - \frac{1}{4}(\eta_{\text{low}}^-)^2 + \mathcal{R}_{\mathbf{u}^0}(\mathbf{w}^0), \tag{30}$$

with arbitrary $s \in \mathbb{R}^+$,

$$\eta_{\text{upp}}^{\pm} \stackrel{\text{def}}{=} \sqrt{s^2 \zeta_{\text{upp}}^2 \pm 2((\mathcal{I}_0 \boldsymbol{\nabla} \mathbf{u}^0, \mathcal{I}_0 \boldsymbol{\nabla} \mathbf{w}^0))_E + s^{-2} \bar{\zeta}_{\text{upp}}^2}, \tag{31}$$

and

$$\eta_{\text{low}}^{\pm} \stackrel{\text{def}}{=} \frac{|\mathcal{R}_{s\mathbf{u}^0 \pm s^{-1}\mathbf{w}^0}(\mathbf{u}^0 + \theta^{\pm}\mathbf{w}^0)|}{\|\mathbf{u}^0 + \theta^{\pm}\mathbf{w}^0\|_{E(\Omega)}}, \tag{32}$$

where ζ_{upp} *and* $\bar{\zeta}_{\text{upp}}$ *are defined by* (15) *and* (27), *respectively*, *and* $\theta^{\pm}$ *is given by*

$$\theta^{\pm} = \frac{\mathcal{B}(\mathbf{u}^0, \mathbf{w}^0)\mathcal{R}_{\mathbf{u}^0}(s\mathbf{u}^0 \pm s^{-1}\mathbf{w}^0) - \mathcal{B}(\mathbf{u}^0, \mathbf{u}^0)\mathcal{R}_{\mathbf{w}^0}(s\mathbf{u}^0 \pm s^{-1}\mathbf{w}^0)}{\mathcal{B}(\mathbf{u}^0, \mathbf{w}^0)\mathcal{R}_{\mathbf{w}^0}(s\mathbf{u}^0 \pm s^{-1}\mathbf{w}^0) - \mathcal{B}(\mathbf{w}^0, \mathbf{w}^0)\mathcal{R}_{\mathbf{u}^0}(s\mathbf{u}^0 \pm s^{-1}\mathbf{w}^0)}. \tag{33}$$

Proof. The outline of the proof is given below; see [6] for details. The error in the quantity of interest can be decomposed as

$$L(\mathbf{e}^0) = \mathcal{B}(\mathbf{e}^0, \mathbf{w}) = \mathcal{B}(\mathbf{e}^0, \bar{\mathbf{e}}^0) + \mathcal{B}(\mathbf{e}^0, \mathbf{w}^0) = \mathcal{B}(s\mathbf{e}^0, s^{-1}\bar{\mathbf{e}}^0) + \mathcal{R}_{\mathbf{u}^0}(\mathbf{w}^0), \tag{34}$$

where $s \in \mathbb{R}^+$ is an, as yet, unspecified positive scaling factor. Now, using a simple property of an inner product, we rewrite the expression (34) as

$$L(\mathbf{e}^0) = \frac{1}{4}\|s\mathbf{e}^0 + s^{-1}\bar{\mathbf{e}}^0\|_{E(\Omega)}^2 - \frac{1}{4}\|s\mathbf{e}^0 - s^{-1}\bar{\mathbf{e}}^0\|_{E(\Omega)}^2 + \mathcal{R}_{\mathbf{u}^0}(\mathbf{w}^0). \tag{35}$$

The first two terms on the right-hand side of (35) can be bounded above by noting that the quantity $s\mathbf{e}^0 \pm s^{-1}\bar{\mathbf{e}}^0$ satisfies

$$\mathcal{B}(s\mathbf{e}^0 \pm s^{-1}\bar{\mathbf{e}}^0, \mathbf{v}) = \mathcal{R}_{s\mathbf{u}^0 \pm s^{-1}\mathbf{w}^0}(\mathbf{v}) \quad \forall\, \mathbf{v} \in \mathbf{V}(\Omega), \tag{36}$$

and hence

$$\|s\mathbf{e}^0 \pm s^{-1}\bar{\mathbf{e}}^0\|_{E(\Omega)} \leq \eta^{\pm}_{\text{upp}}, \tag{37}$$

with

$$\begin{aligned} \eta^{\pm}_{\text{upp}} &\stackrel{\text{def}}{=} \left\{ \int_\Omega \mathcal{I}_0 \boldsymbol{\nabla}(s\mathbf{u}^0 \pm s^{-1}\mathbf{w}^0) : \mathbf{E}\mathcal{I}_0 \boldsymbol{\nabla}(s\mathbf{u}^0 \pm s^{-1}\mathbf{w}^0)\, d\mathbf{x} \right\}^{1/2} \\ &= \left\{ s^2\zeta^2_{\text{upp}} \pm 2((\mathcal{I}_0\boldsymbol{\nabla}\mathbf{u}^0, \mathcal{I}_0\boldsymbol{\nabla}\mathbf{w}^0))_E + s^{-2}\bar{\zeta}^2_{\text{upp}} \right\}^{1/2}. \end{aligned} \tag{38}$$

To obtain a lower bound on the quantity $s\mathbf{e}^0 \pm s^{-1}\bar{\mathbf{e}}^0$, we note that

$$\|s\mathbf{e}^0 \pm s^{-1}\bar{\mathbf{e}}^0\|_{E(\Omega)} = \|\mathcal{R}_{s\mathbf{u}^0 \pm s^{-1}\mathbf{w}^0}\|_{E'(\Omega)} \geq \frac{|\mathcal{R}_{s\mathbf{u}^0 \pm s^{-1}\mathbf{w}^0}(\mathbf{v})|}{\|\mathbf{v}\|_{E(\Omega)}}, \tag{39}$$

for any $\mathbf{v} \in \mathbf{V}(\Omega)\backslash\{\mathbf{0}\}$. A linear combination of $\mathbf{u}^0$ and $\mathbf{w}^0$ of the form $\mathbf{v} = \mathbf{u}^0 + \theta^{\pm}\mathbf{w}^0$, $\theta^{\pm} \in \mathbb{R}$, is then used in the above expression to obtain the best possible lower bound. The value $\theta^{\pm}$ is found by a simple extremization process. The third term $\mathcal{R}_{\mathbf{u}^0}(\mathbf{w}^0)$ depends only on known quantities. ■

It can be shown that the optimal value of the scaling factor s is given by

$$s^* = \sqrt{\|\bar{\mathbf{e}}^0\|_{E(\Omega)}/\|\mathbf{e}^0\|_{E(\Omega)}}.$$

However, since $\bar{\mathbf{e}}^0$ and $\mathbf{e}^0$ are not known exactly, we use

$$s^* = \sqrt{\bar{\zeta}_{\text{upp}}/\zeta_{\text{upp}}}.$$

Also, in our numerical experiments, we employ the following *estimates* of the modeling error in the quantity of interest:

$$L(\mathbf{e}^0) \approx \eta_{\text{est,upp}} \stackrel{\text{def}}{=} \frac{1}{4}(\eta^+_{\text{upp}})^2 - \frac{1}{4}(\eta^-_{\text{upp}})^2 + \mathcal{R}_{\mathbf{u}^0}(\mathbf{w}^0), \tag{40}$$

and

$$L(\mathbf{e}^0) \approx \eta_{\text{est,low}} \stackrel{\text{def}}{=} \frac{1}{4}(\eta^+_{\text{low}})^2 - \frac{1}{4}(\eta^-_{\text{low}})^2 + \mathcal{R}_{\mathbf{u}^0}(\mathbf{w}^0). \tag{41}$$

An important feature of the theorem above is that the elasticity tensor $\mathbf{E}^0$ need not be a constant function; it need only satisfy the uniform ellipticity and symmetry conditions.

FIG. 4. Plots of the (a) ε_{11} and (b) ε_{22} components of the strain tensor $\varepsilon(\mathbf{w}^0)$ for the quantity of interest L_2.

3.2. *Modeling Error in Quantities of Interest for Admissible Functions*

We now demonstrate how to obtain bounds on the quantity $L(\mathbf{u}-\mathbf{z})$ for admissible functions $\mathbf{z} \in \mathbf{V}(\Omega)$, $\mathbf{z} \neq \mathbf{0}$, where $L \in \mathbf{V}'(\Omega)$ denotes a quantity of interest. We first define, for $s \in \mathbb{R}^+$, the functional $\mathcal{J}_s^{\pm} : \mathbf{V}(\Omega) \to \mathbb{R}$,

$$\mathcal{J}_s^{\pm}(\mathbf{v}) \stackrel{\text{def}}{=} \frac{1}{2}\mathcal{B}(\mathbf{v},\mathbf{v}) - (s\mathcal{F} \pm s^{-1}L)(\mathbf{v}), \quad \mathbf{v} \in \mathbf{V}(\Omega). \tag{42}$$

It is easy to see that:

- The functional $\mathcal{J}_s^{\pm}$ has a unique minimizer $\mathcal{X}_s^{\pm}$ that satisfies

$$\mathcal{B}(\chi_s^{\pm}, \mathbf{v}) = (s\mathcal{F} \pm s^{-1}L)(\mathbf{v}), \quad \forall\, \mathbf{v} \in \mathbf{V}(\Omega). \tag{43}$$

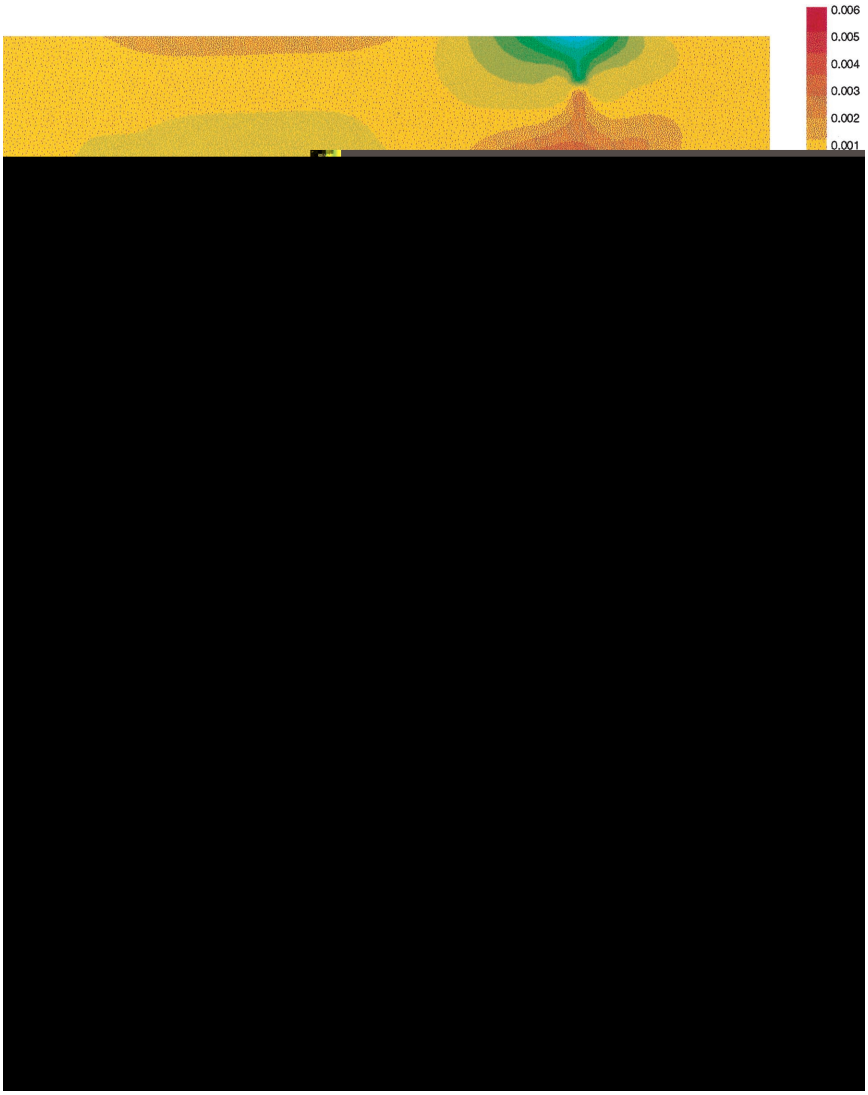

FIG. 5. Plots of the (a) ε_{11} and (b) ε_{22} components of the strain tensor $\varepsilon(\mathbf{w}^0)$ for the quantity of interest L_3.

Moreover,

$$\chi_s^{\pm} \equiv s\mathbf{u} \pm s^{-1}\mathbf{w}, \tag{44}$$

where $\mathbf{u}$ is the unique solution to (7) and $\mathbf{w}$ is the unique solution to (22).

- If $\mathbf{v} \in \mathbf{V}(\Omega)$, $\mathbf{v} \neq 0$, then, in the spirit of Corollary 2.1, we have

$$\eta_{\text{low}}^{\pm}(\mathbf{v}) \leq \|(s\mathbf{u} \pm s^{-1}\mathbf{w}) - \mathbf{v}\|_{\text{E}(\Omega)} = \|\chi_s^{\pm} - \mathbf{v}\|_{\text{E}(\Omega)} \leq \eta_{\text{upp}}^{\pm}(\mathbf{v}), \tag{45}$$

where

$$\eta_{\text{upp}}^{\pm}(\mathbf{v}) \stackrel{\text{def}}{=} \sqrt{2(\mathcal{J}_s^{\pm}(\mathbf{v}) - \mathcal{J}_s^{\pm}(s\mathbf{u}^0 \pm s^{-1}\mathbf{w}^0)) + (\eta_{\text{upp}}^{\pm})^2}, \tag{46}$$

and

$$\eta^{\pm}_{\text{low}}(\mathbf{v}) \stackrel{\text{def}}{=} \frac{|(s\mathcal{F} \pm s^{-1}L)(\mathbf{v}) - \mathcal{B}(\mathbf{v},\mathbf{v})|}{\|\mathbf{v}\|_{E(\Omega)}}, \tag{47}$$

where $\eta^{\pm}_{\text{upp}}$ is as defined in (31).

These preliminaries bring us to the following result:

THEOREM 3.2. *Let* $\mathbf{u}^0$ *and* $\mathbf{w}^0$ *be the solutions to problems* (9) *and* (23)*, respectively. Let* $\mathbf{z} \in \mathbf{V}(\Omega)$, $\mathbf{z} \neq 0$, *and denote the quantity of interest by* $L \in \mathbf{V}'(\Omega)$. *Moreover, let* $s \in \mathbb{R}^+$. *Then, the quantity* $L(\mathbf{u} - \mathbf{z})$ *can be bounded above and below,*

$$\eta_{\text{low}}(\mathbf{z}) \leq L(\mathbf{u} - \mathbf{z}) \leq \eta_{\text{upp}}(\mathbf{z}) \tag{48}$$

with

$$\eta_{\text{low}}(\mathbf{z}) \stackrel{\text{def}}{=} \frac{1}{4}(\eta^{+}_{\text{low}}(s\mathbf{z} + s^{-1}\mathbf{w}^0))^2 - \frac{1}{4}(\eta^{-}_{\text{upp}}(s\mathbf{z} - s^{-1}\mathbf{w}^0))^2 + \mathcal{F}(\mathbf{w}^0) - \mathcal{B}(\mathbf{z},\mathbf{w}^0), \tag{49}$$

and

$$\eta_{\text{upp}}(\mathbf{z}) \stackrel{\text{def}}{=} \frac{1}{4}(\eta^{+}_{\text{upp}}(s\mathbf{z} + s^{-1}\mathbf{w}^0))^2 - \frac{1}{4}(\eta^{-}_{\text{low}}(s\mathbf{z} - s^{-1}\mathbf{w}^0))^2 + \mathcal{F}(\mathbf{w}^0) - \mathcal{B}(\mathbf{z},\mathbf{w}^0), \tag{50}$$

and $\eta^{\pm}_{\text{upp}}(\mathbf{v})$ *and* $\eta^{\pm}_{\text{low}}(\mathbf{v})$, $\mathbf{v} \in \mathbf{V}(\Omega)$,

Later, we will also use the following estimates of the quantity $L(\mathbf{u}-\mathbf{z})$:

$$L(\mathbf{u}-\mathbf{z}) \approx \eta^z_{\text{est,upp}} \stackrel{\text{def}}{=} \frac{1}{4}(\eta^+_{\text{upp}}(s\mathbf{z}+s^{-1}\mathbf{w}^0))^2 - \frac{1}{4}(\eta^-_{\text{upp}}(s\mathbf{z}-s^{-1}\mathbf{w}^0))^2 + \mathcal{F}(\mathbf{w}^0) - \mathcal{B}(\mathbf{z},\mathbf{w}^0), \tag{55}$$

and

$$L(\mathbf{u}-\mathbf{z}) \approx \eta^z_{\text{est,low}} \stackrel{\text{def}}{=} \frac{1}{4}(\eta^+_{\text{low}}(s\mathbf{z}+s^{-1}\mathbf{w}^0))^2 - \frac{1}{4}(\eta^-_{\text{low}}(s\mathbf{z}-s^{-1}\mathbf{w}^0))^2 + \mathcal{F}(\mathbf{w}^0) - \mathcal{B}(\mathbf{z},\mathbf{w}^0). \tag{56}$$

Remark. The definitions of the functionals L can, in some cases, be extended to nonlinear quantities of interest through linearization. For example, if one is interested in the squared root-mean-square norm (the L^2 norm squared) of $\mathbf{u}$ over a subdomain $\omega \subset \Omega$, then the nonlinear quantity of interest is

$$\mathcal{N}(\mathbf{u}) = \int_\omega \mathbf{u}\cdot\mathbf{u}\, d\mathbf{x}. \tag{57}$$

The modeling error in this quantity of interest is

$$\begin{aligned}\mathcal{N}(\mathbf{u}) - \mathcal{N}(\mathbf{u}^0) &= \int_\omega (\mathbf{u}\cdot\mathbf{u} - \mathbf{u}^0\cdot\mathbf{u}^0)\, d\mathbf{x} \\ &= \int_\omega ((\mathbf{u}^0+\mathbf{e}^0)\cdot(\mathbf{u}^0+\mathbf{e}^0) - \mathbf{u}^0\cdot\mathbf{u}^0)\, d\mathbf{x} \\ &= 2\int_\omega \mathbf{u}^0\cdot\mathbf{e}^0\, d\mathbf{x} + \int_\omega \mathbf{e}^0\cdot\mathbf{e}^0\, d\mathbf{x} \\ &\approx 2\int_\omega \mathbf{u}^0\cdot\mathbf{e}^0\, d\mathbf{x}. \end{aligned} \tag{58}$$

Then the linearized quantity of interest is given by $L(\mathbf{v}) = 2\int_\omega \mathbf{u}^0\cdot\mathbf{v}\, d\mathbf{x}$.

4. GOAL-ORIENTED ADAPTIVE MODELING

One way to overcome the loss of fine-scale information due to regularization techniques is to use the regularized solution as a starting point in a procedure that adaptively improves the quality of the solution. Such procedures are common in the context of finite elements where a coarse mesh solution is used as a starting point and is adaptively improved upon by refining the mesh. Here, we are concerned with adapting the model of the microstructure itself. We begin this section by describing a goal-oriented strategy for model adaptation for a given quantity of interest. We then present an algorithm based on this strategy.

4.1. *Adaptive Modeling Strategy*

Our strategy for adapting the material model based on modeling error in a quantity of interest $L \in \mathbf{V}'(\Omega)$ consists of:

1. Solution of the regularized problems (9) and (23) for $\mathbf{u}^0$ and $\mathbf{w}^0$, respectively.

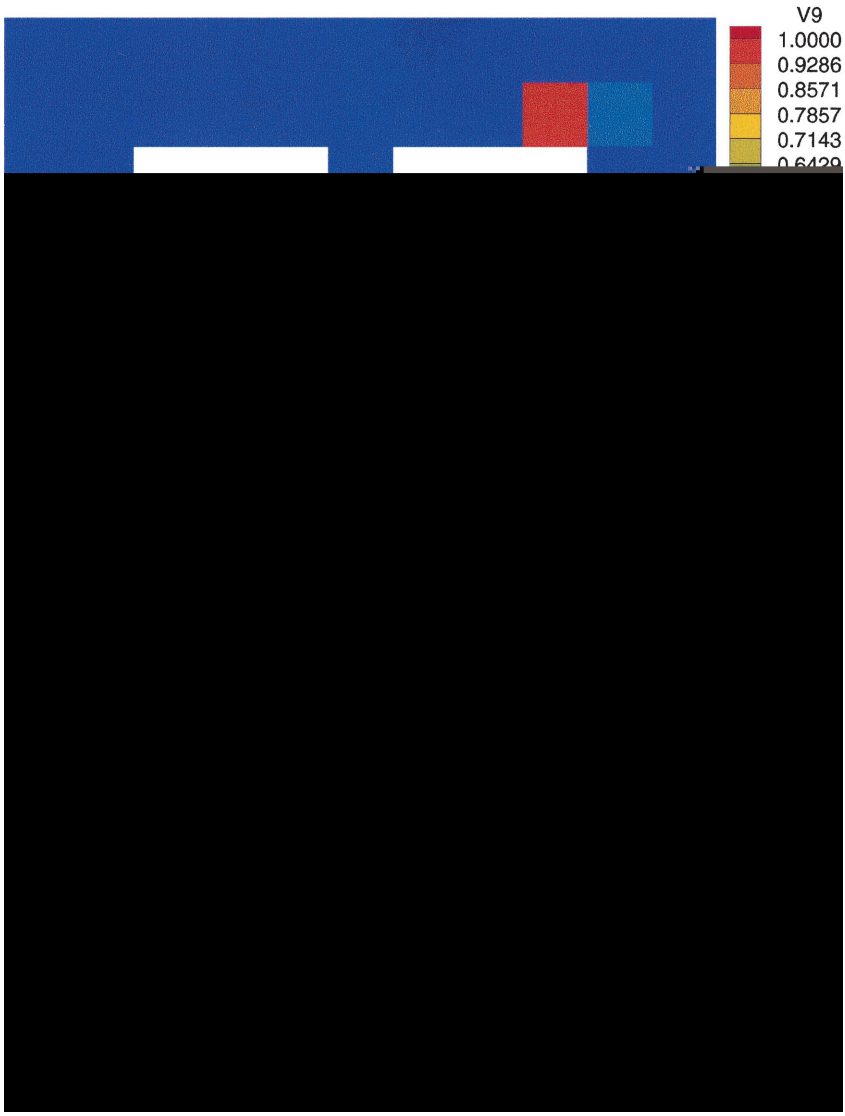

FIG. 6. Distribution of the quantities (a) $\bar{\zeta}_{k,\mathrm{upp}}$ and (b) β_k, normalized with respect to the maximum, for the quantity of interest L_1.

2. Estimation of the modeling error $L(\mathbf{u}-\mathbf{u}^0)$ in the quantity of interest using Theorem 3.1.

3. If required, enhancement of the regularized solution $\mathbf{u}^0$ by taking into account the fine-scale material features over a "region of influence."

Let us elaborate further on the third part of our strategy. Suppose $\Omega_L \subset \Omega$ is determined to be (in a fashion to be described shortly) the region where the finescale elasticity tensor $\mathbf{E}$ most influences the quantity of interest L. We propose solving a problem on Ω_L with the regularized solution $\mathbf{u}^0$ providing the boundary conditions. More precisely, define

$$\Gamma_{L_t} \stackrel{\mathrm{def}}{=} \partial\Omega_L \cap \Gamma_t, \quad \Gamma_{L_u} \stackrel{\mathrm{def}}{=} \partial\Omega_L \backslash \Gamma_{L_t}. \tag{59}$$

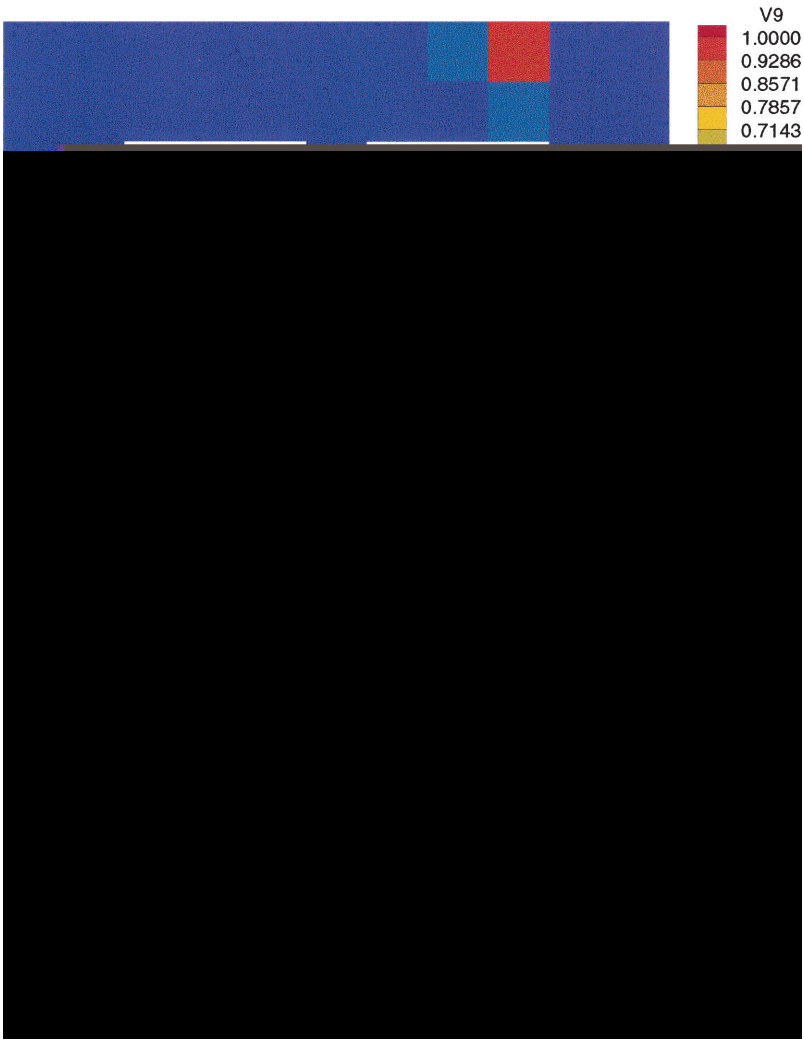

FIG. 7. Distribution of the quantities (a) $\bar{\zeta}_{k,\text{upp}}$ and (b) β_k, normalized with respect to the maximum, for the quantity of interest L_2.

Define the local function space on Ω_L as

$$\mathbf{V}(\Omega_L) = \{\mathbf{v} \in \mathbf{V}(\Omega), \mathbf{v} = \mathbf{0} \text{ on } \Omega \backslash \overline{\Omega_L}, \mathbf{v}|_{\Gamma_{L_u}} = \mathbf{0}\}. \tag{60}$$

Next, an extension operator $\mathcal{E}_L : \mathbf{V}(\Omega_L) \to \mathbf{V}(\Omega)$ is introduced, defined by

$$\mathbf{v}_L \in \mathbf{V}(\Omega_L), \mathcal{E}_L(\mathbf{v}_L) = \mathbf{v} \text{ such that } \mathbf{v}|_{\Omega_L} = \mathbf{v}_L, \mathbf{v}|_{\Omega \backslash \Omega_L} = \mathbf{0}. \tag{61}$$

The restriction of the regularized solution $\mathbf{u}^0$ to the domain of influence Ω_L is defined as $\mathbf{u}_L^0 : \mathbf{u}_L^0 \overset{\text{def}}{=} \mathbf{u}^0|_{\Omega_L}$. Then $\tilde{\mathbf{u}}_L$ is sought as the solution to the following weak boundary value problem:

$$\begin{gathered} \text{Find } \tilde{\mathbf{u}}_L \in \left\{\mathbf{u}_L^0\right\} + \mathbf{V}(\Omega_L) \text{ such that} \\ \mathcal{B}_L(\tilde{\mathbf{u}}_L, \mathbf{v}_L) = \mathcal{F}_L(\mathbf{v}_L) \quad \forall \mathbf{v}_L \in \mathbf{V}(\Omega_L), \end{gathered} \tag{62}$$

where the bilinear and linear forms are defined as

$$\mathcal{B}_L(\tilde{\mathbf{u}}_L, \mathbf{v}_L) \stackrel{\text{def}}{=} \int_{\Omega_L} \boldsymbol{\nabla}\mathbf{v}_L : \mathbf{E}\boldsymbol{\nabla}\tilde{\mathbf{u}}_L \, d\mathbf{x}, \tag{63}$$

and

$$\mathcal{F}_L(\mathbf{v}_L) \stackrel{\text{def}}{=} \int_{\Omega_L} \mathbf{f} \cdot \mathbf{v}_L \, d\mathbf{x} + \int_{\Gamma_{L_t}} \mathbf{t} \cdot \mathbf{v}_L \, d\mathbf{s}, \tag{64}$$

respectively. Thus, $\tilde{\mathbf{u}}_L$ is a perturbation on Ω_L that takes into account the fine-scale microstructure. Moreover, it equals the primal regularized solution $\mathbf{u}^0$ on the Γ_{L_u} portion of its boundary. Using the extension operator introduced earlier, we arrive at a *locally enhanced* function $\tilde{\mathbf{u}} \in \mathbf{V}(\Omega)$ defined as

$$\tilde{\mathbf{u}} \stackrel{\text{def}}{=} \mathbf{u}^0 + \mathcal{E}_L\left(\tilde{\mathbf{u}}_L - \mathbf{u}_L^0\right). \tag{65}$$

We now make two observations:

- The locally enhanced solution $\tilde{\mathbf{u}} \in \mathbf{V}(\Omega)$ is an admissible function and satisfies the kinematic constraint $\tilde{\mathbf{u}}|_{\Gamma_u} = \mathbf{0}$, even though it is not the solution to a global problem posed on Ω.
- The modeling error in the quantity of interest L corresponding to the perturbed solution is $L(\mathbf{u}) - L(\tilde{\mathbf{u}}) = L(\mathbf{u} - \tilde{\mathbf{u}})$. This quantity can be bounded above and below using Theorem 3.2.

We now propose a technique to determine the "domain of influence" Ω_L. We consider a nonoverlapping partition $\mathcal{P}$ of the domain Ω into cells Θ_k, $1 \le k \le N(\mathcal{P})$, where $N(\mathcal{P})$ is the total number of cells in the partition. Define

$$\begin{aligned} \zeta_{k,\text{upp}} &\stackrel{\text{def}}{=} \left\{ \int_{\Theta_k} \mathcal{I}_0 \boldsymbol{\nabla}\mathbf{u}^0 : \mathbf{E}\mathcal{I}_0 \boldsymbol{\nabla}\mathbf{u}^0 \, d\mathbf{x} \right\}^{\frac{1}{2}} \\ \bar{\zeta}_{k,\text{upp}} &\stackrel{\text{def}}{=} \left\{ \int_{\Theta_k} \mathcal{I}_0 \boldsymbol{\nabla}\mathbf{w}^0 : \mathbf{E}\mathcal{I}_0 \boldsymbol{\nabla}\mathbf{w}^0 \, d\mathbf{x} \right\}^{\frac{1}{2}}, \end{aligned} \tag{66}$$

and note that

$$\zeta_{\text{upp}}^2 = \sum_{k=1}^{N(\mathcal{P})} \zeta_{k,\text{upp}}^2, \quad \bar{\zeta}_{\text{upp}}^2 = \sum_{k=1}^{N(\mathcal{P})} \bar{\zeta}_{k,\text{upp}}^2, \tag{67}$$

where ζ_{upp} and $\bar{\zeta}_{\text{upp}}$ were introduced in (15) and (27), respectively. Next, note that the proof of Theorem 3.1 (see [6]) is based on the decomposition

$$L(\mathbf{e}^0) = \mathcal{B}(\mathbf{e}^0, \bar{\mathbf{e}}^0) + \mathcal{B}(\mathbf{e}^0, \mathbf{w}^0), \tag{68}$$

which implies that

$$|L(\mathbf{e}^0)| \le \beta \stackrel{\text{def}}{=} \zeta_{\text{upp}} \bar{\zeta}_{\text{upp}} + \zeta_{\text{upp}} \|\mathbf{w}^0\|_{E(\Omega)}. \tag{69}$$

This suggests that the cells k in which the quantity

$$\beta_k \stackrel{\text{def}}{=} \zeta_{k,\text{upp}}\bar{\zeta}_{k,\text{upp}} + \zeta_{k,\text{upp}}\|\mathbf{w}^0\|_{E(\Theta_k)} \tag{70}$$

exceeds a tolerance can be picked to constitute the domain of influence Ω_L.

4.2. *The Goal-Oriented Adaptive Local Solution Algorithm (GOALS)*

We begin by considering quantities of interest of the type

$$L(\mathbf{v}) = \int_\omega l(\mathbf{v})\, d\mathbf{x}, \quad \omega \subset \Omega, \tag{71}$$

where l is a linear map: $l : \mathbf{V}(\Omega) \to L^1_{\text{loc}}(\Omega)$. Our algorithm can be easily modified to accommodate quantities of interest of other types. The GOALS algorithm can now be stated as follows:

Step 1: Initialization. Given the initial data Ω, Γ_u, Γ_t, $\mathbf{E}$, $\mathbf{f}$, and $\mathbf{t}$, construct a nonoverlapping partition of the domain $\mathcal{P} = \{\Theta_k\}, k = 1.2 \ldots N(\mathcal{P})$. Specify error tolerance parameters α_{TOL} and δ_{TOL}, $0 < \delta_{\text{TOL}} < 1$.

Step 2: Regularization. Compute the homogenized elasticity tensor $\mathbf{E}^0$. Solve the primal regularized problem (9) for $\mathbf{u}^0$ and the adjoint regularized problem (23) for $\mathbf{w}^0$.

Step 3: Modeling error estimation. Compute error indicators ζ_k, $\bar{\zeta}_k$, and β_k for $1 \le k \le N(\mathcal{P})$, using (66) and (70). Estimate the modeling error in the quantity of interest using Theorem 3.1. Denote this estimate by η_{est}.

Step 4: Tolerance test. If $\eta_{\text{est}} \le \alpha_{\text{TOL}} \times L(\mathbf{u}^0)$, STOP.

Step 5: Domain of influence. Determine initial guess for "domain of influence" Ω_L as all the cells that intersect ω, the region over which the quantity of interest is defined:

$$\overline{\Omega_L} = \overline{\cup_{j\in\mathcal{J}}\Theta_j} \quad \mathcal{J} \stackrel{\text{def}}{=} \{j : \Theta_j \cap \omega \neq \emptyset\}. \tag{72}$$

Compute the quantities ζ_L, $\bar{\zeta}_L$, and β_L:

$$\zeta_L \stackrel{\text{def}}{=} \left\{\sum_{k\in\mathcal{J}} \zeta^2_{k,\text{upp}}\right\}^{\frac{1}{2}}, \quad \bar{\zeta}_L \stackrel{\text{def}}{=} \left\{\sum_{k\in\mathcal{J}} \bar{\zeta}^2_{k,\text{upp}}\right\}^{\frac{1}{2}}, \quad \beta_L \stackrel{\text{def}}{=} \zeta_L\bar{\zeta}_L + \zeta_L\|\mathbf{w}^0\|_{E(\Omega_L)}. \tag{73}$$

Step 6: Update domain of influence. Determine the "bad neighbors" of Ω_L; i.e., if $\beta_i > \delta_{\text{TOL}} \times \beta_L$, mark Θ_i as bad and update Ω_L:

$$\Omega_L \leftarrow \Omega_L \cup \{\text{bad neighbors}\}. \tag{74}$$

Update the quantities ζ_L, $\bar{\zeta}_L$, and β_L.

Step 7: Solution of local problem. Solve local problem (62) on Ω_L for $\tilde{\mathbf{u}}_L$. Construct the locally enhanced solution $\tilde{\mathbf{u}} \in \mathbf{V}(\Omega)$ using (65).

Step 8: Estimate modeling error. Estimate the modeling error $L(\mathbf{u} - \tilde{\mathbf{u}})$ using Theorem 3.2 and denote the estimate by η_{est}. If $\eta_{\text{est}} \le \alpha_{\text{TOL}} \times L(\tilde{\mathbf{u}})$, STOP. Else, GOTO Step 6.

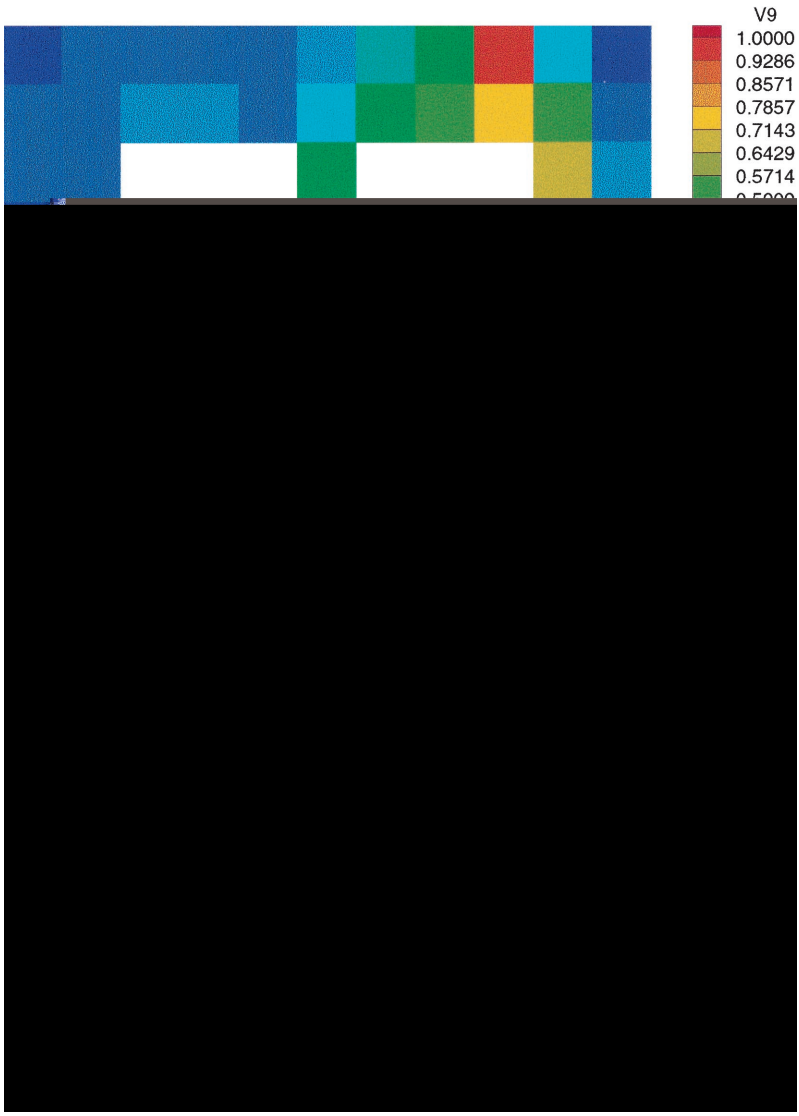

FIG. 8. Distribution of the quantities (a) $\bar{\zeta}_{k,\mathrm{upp}}$ and (b) β_k, normalized with respect to the maximum, for the quantity of interest L_3.

In many applications, the decay of local effects may be very fast, meaning that Ω_L is often small in comparison with Ω

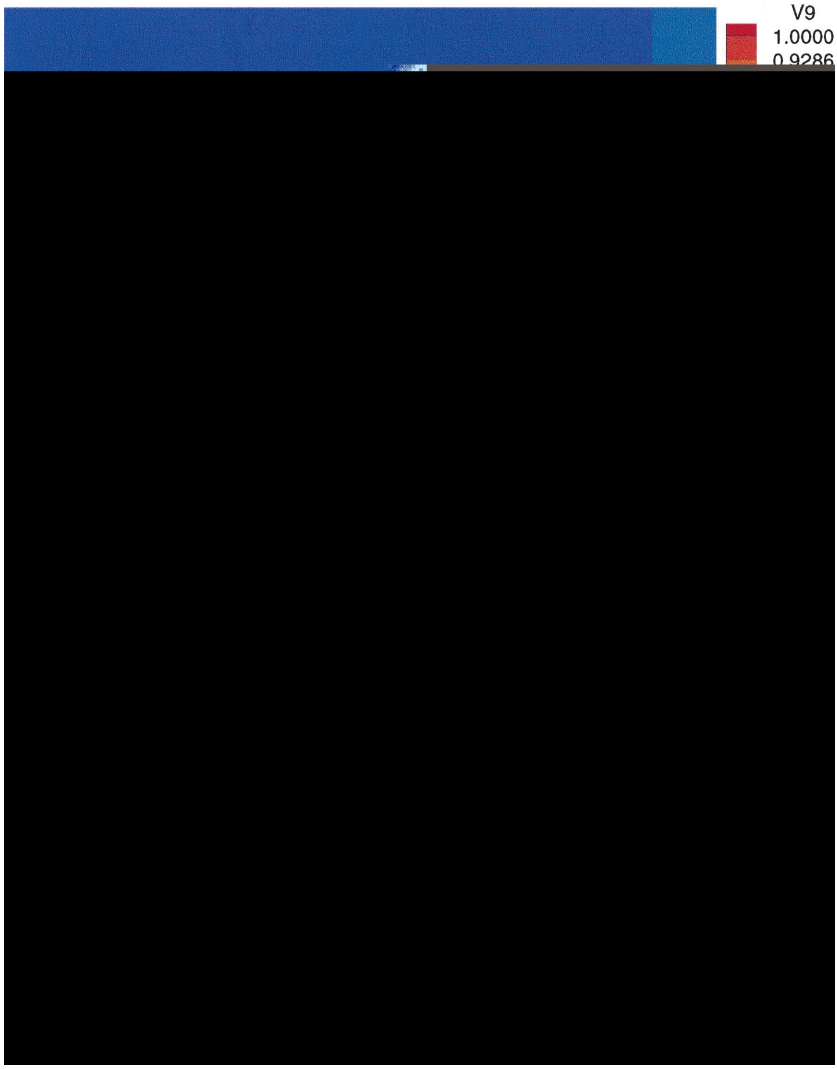

FIG. 9. Distribution of the quantities (a) $\bar{\zeta}_{k,\text{upp}}$ and (b) β_k, normalized with respect to the maximum, for the quantity of interest L_4.

material properties are taken to be ($E = 100.0$ MPa, $\nu = 0.2$) for the matrix material and ($E = 1000.0$ MPa, $\nu = 0.2$) for the inclusions, where E is the Young's modulus and ν is the Poisson's ratio. Plane strain conditions are assumed to hold.

The domain is partitioned into $N(\mathcal{P}) = 42$ cells as indicated by the dashed lines in Fig. 1 (Step 1 of the GOALS algorithm). Because of the lack of microstructural periodicity, the homogenized properties of the domain are taken to be the average of the Hashin–Shtrikman upper and lower bounds [3] (Step 2).

To evaluate the accuracy and effectivity of various bounds, we compute numerical approximations of reference fine-scale solutions $\mathbf{u}$ and $\mathbf{w}$, since these are not known exactly. To reduce the influence of approximation error on the results, it is important that the numerical approximations to the fine-scale functions, as well as those to the homogenized functions $\mathbf{u}^0$ and $\mathbf{w}^0$, be computed with very high accuracy. Toward this end, we perform

all computations using the h-p adaptive finite-element code ProPHLEX [2]. Sample h-p meshes are shown later in this section.

5.2. *Domains of Influence*

Evidently, the amount of microscale information necessary to accurately predict a quantity of interest depends on the quantity of interest itself. A qualitative approach to determining the domain of influence of a quantity of interest is now described. Consider the following quantities of interest:

$$\begin{aligned} L_1(\mathbf{v}) &= \frac{1}{|\omega_1|}\int_{\omega_1}\sigma_{11}(\mathbf{v})\,d\mathbf{x} = \frac{1}{|\omega_1|}\int_{\omega_1}\left(C_1\frac{\partial v_1}{\partial x}+C_2\frac{\partial v_2}{\partial y}\right)d\mathbf{x},\\ L_2(\mathbf{v}) &= \frac{1}{|\omega_2|}\int_{\omega_2}\varepsilon_{22}(\mathbf{v})\,d\mathbf{x} = \frac{1}{|\omega_2|}\int_{\omega_2}\frac{\partial v_2}{\partial y}\,d\mathbf{x},\\ L_3(\mathbf{v}) &= \int_{\omega_2} k_\epsilon(\mathbf{x};\mathbf{x}_0)v_2(\mathbf{x})\,d\mathbf{x}. \end{aligned} \tag{75}$$

The first quantity of interest L_1 represents the σ_{11} component of the stress tensor averaged over the inclusion ω_1, shown in Fig. 1, with appropriate material constants C_1 and C_2. The second quantity of interest L_2 represents the ε_{22} component of the strain tensor averaged over the inclusion ω_2.

The third quantity of interest is a *mollification* of the y component of the displacement vector over the inclusion ω_2. The use of mollification is necessitated by the fact that one cannot refer to the point-wise values of functions in $\mathbf{V}(\Omega)$. The mollifier kernel $k_\epsilon(\cdot;\mathbf{x}_0)$ is an infinitely smooth function and its support is a ball of radius ϵ centered at $\mathbf{x}_0$ (denoted $B_\epsilon(\mathbf{x}_0)$). We choose $\mathbf{x}_0$ and ϵ so that $\omega_2 = B_\epsilon(\mathbf{x}_0)$. The mollifier kernel has the following properties [5]:

- It has continuous derivatives of all orders on $\mathbb{R}^N$.
- $k_\epsilon(\mathbf{x};\mathbf{x}_0) = 0$ for $|\mathbf{x}-\mathbf{x}_0| \geq \epsilon$ and $k_\epsilon(\mathbf{x};\mathbf{x}_0) > 0$ for $|\mathbf{x}-\mathbf{x}_0| < \epsilon$.
- $\int_{B_\epsilon(\mathbf{x}_0)} k_\epsilon(\mathbf{x},\mathbf{x}_0)\,d\mathbf{x} = 1$.

First, the primal homogenized solution $\mathbf{u}^0$ is computed by solving (9). The modeling error indicators for the primal problem, $\zeta_{k,\text{upp}}$, are then computed using (66). These quantities are shown in Fig. 2.

Next, the homogenized influence functions $\mathbf{w}^0$ corresponding to the three quantities of interest defined above are computed by solving (9). In Figs. 3, 4, and 5, we show the ε_{11} and ε_{22} components of the strain tensor $\varepsilon(\mathbf{w}^0)$ for the quantities L_1, L_2, and L_3, respectively. Recall that it is the strain tensor of $\mathbf{w}^0$ that appears in the various expressions for the modeling error in a quantity of interest. It is seen that, in the case of L_1 and L_2, the components of $\varepsilon(\mathbf{w}^0)$ are small everywhere except in a small neighborhood of the region of interest. For the quantity of interest L_3, the strains are nonzero over a larger portion of the domain Ω.

The modeling error indicators for the adjoint problems, $\bar{\zeta}_{k,\text{upp}}$ and β_k, are computed using (66) and (70). The indicator β_k roughly represents the magnitude of the contribution (or the influence) of a cell to the modeling error in the quantity of interest, and its distribution over Ω provides a qualitative description of the domain of influence of the quantity of interest.

The quantities $\bar{\zeta}_{k,\text{upp}}$ and β_k for L_1, L_2, L_3 are shown in Figs. 6–8. A major difference between the distribution of the primal and the adjoint error indicators is that the primal

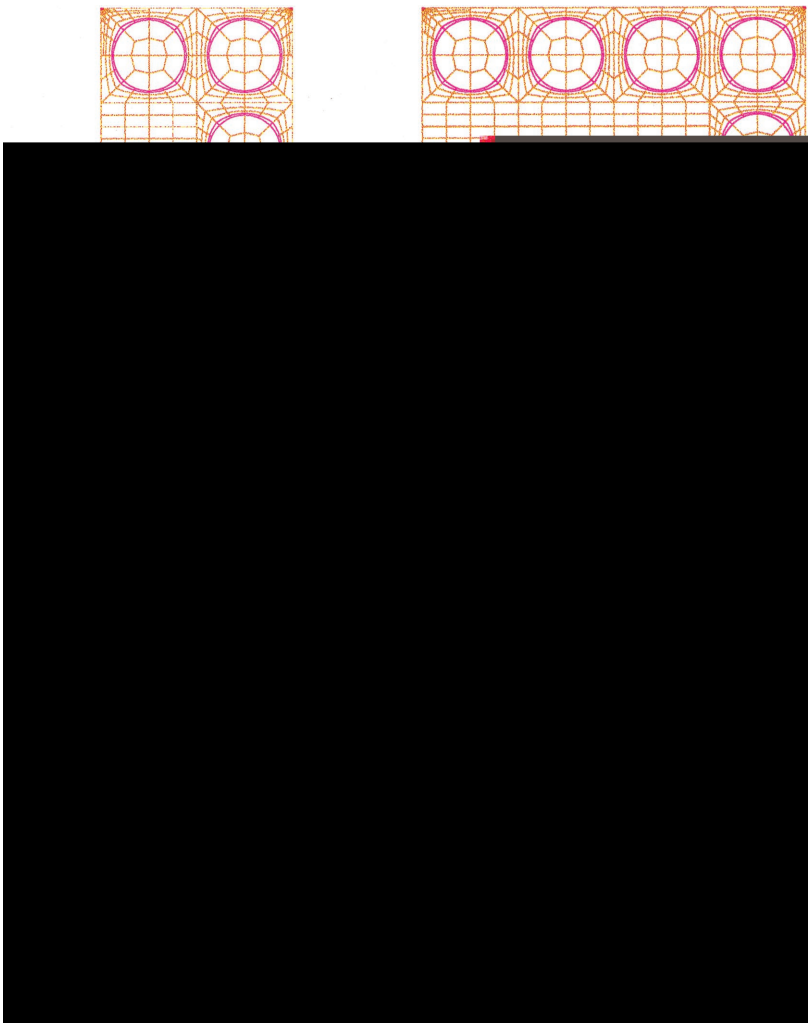

FIG. 10. The h-p meshes for the sequence of domains of influence and the resulting modeling errors in the quantity of interest L_4: (a) Ω_L^0, (b) Ω_L^1, (c) Ω_L^2, and (d) Ω_L^3.

indicators are global in nature, whereas the adjoint indicators for L_1 and L_2 are markedly local. Note that the domain of influence of the quantity of interest L_3 is much larger than it is for L_1 and L_2. This indicates that more fine-scale information is required to accurately predict local displacements than is required to predict local stresses or strains. Also, for the quantity of interest L_3, the computation of the indicators was repeated with ϵ, the mollification kernel radius, reduced by half. The change in the distribution of the normalized error indicators was found to be negligible, suggesting that the nonlocality of the distribution of these error indicators is quite insensitive to ϵ.

5.3. *Error Estimation and Adaptive Modeling*

Here, the adaptive modeling strategy proposed earlier is used to determine a material model that accurately predicts the quantity of interest

$$L_4(\mathbf{v}) = \frac{1}{|\omega_3|}\int_{\omega_3} \sigma_{11}(\mathbf{v})\, d\mathbf{x} = \frac{1}{|\omega_3|}\int_{\omega_3}\left(C_1\frac{\partial v_1}{\partial x} + C_2\frac{\partial v_2}{\partial y}\right) d\mathbf{x}, \tag{76}$$

TABLE I
Effectivity Indices of the Estimates Associated with the Primal Problem

Error estimate	Effectivity index
$\dfrac{\zeta_{\text{upp}}}{\|\mathbf{u}-\mathbf{u}^0\|_{E(\Omega)}}$	1.085
$\dfrac{\zeta_{\text{low}}}{\|\mathbf{u}-\mathbf{u}^0\|_{E(\Omega)}}$	0.494

where ω_3 is the region occupied by the inclusion indicated in Fig. 1. This quantity of interest is the average of the σ_{11} component of the stress tensor on the inclusion ω_3 (with appropriate material constants C_1 and C_2).

After the homogenized influence function $\mathbf{w}^0$ is computed, the modeling error indicators $\bar{\zeta}_{k,\text{upp}}$, and β_k are computed using (66) and (70). In Fig. 9 we show the normalized quantities $\bar{\zeta}_{k,\text{upp}}$, and β_k, $1 \le k \le 42$. Again, note the highly local nature of the error indicators $\bar{\zeta}_{k,\text{upp}}$ and β_k.

To assess the quality of the error bounds and estimates computed in this step of the GOALS algorithm, we use the notion of an *effectivity index*. For a given error estimate, the effectivity index is defined as the ratio of the estimated error to the true error. In our case, we compute the "true error" using the reference solutions $\mathbf{u}$ and $\mathbf{w}$. The closer the effectivity index is to unity, the better the quality of the estimate. Thus, the effectivity index of the upper bound on the homogenization error ζ_{upp} introduced in (15) is $\zeta_{\text{upp}}/\|\mathbf{u}-\mathbf{u}^0\|_{E(\Omega)}$. First, the effectivity indices of the estimates corresponding to the primal problem are shown Table I. We see that the upper bound ζ_{upp} is very close to true homogenization error $\|\mathbf{u}-\mathbf{u}^0\|_{E(\Omega)}$, whereas the lower bound is inefficient.

The effectivity indices of the estimates associated with the adjoint problem are next shown in Table II. For the adjoint problem, both the upper and lower bounds on $\|\mathbf{w}-\mathbf{w}^0\|_{E(\Omega)}$ are seen to be accurate. The bounds η_{upp} and η_{low} on the modeling error in the quantity of interest are far from unity as expected; for a detailed analysis of the accuracy of these

TABLE II
Effectivity Indices of the Estimates Associated with the Adjoint Problem Corresponding to the Quantity of Interest *L*

Error estimate	Effectivity index
$\dfrac{\bar{\zeta}_{\text{upp}}}{\|\mathbf{w}-\mathbf{w}^0\|_{E(\Omega)}}$	1.123
$\dfrac{\bar{\zeta}_{\text{low}}}{\|\mathbf{w}-\mathbf{w}^0\|_{E(\Omega)}}$	0.994
$\dfrac{\eta_{\text{upp}}}{L(\mathbf{e}^0)}$	−162.7
$\dfrac{\eta_{\text{low}}}{L(\mathbf{e}^0)}$	161.4
$\dfrac{\eta_{\text{est,low}}}{L(\mathbf{e}^0)}$	0.709
$\dfrac{\eta_{\text{est,upp}}}{L(\mathbf{e}^0)}$	−2.028

bounds, see [6]. We see that the estimate $\eta_{\text{est,low}}$ alone has a reasonable effectivity index. In our experience, this estimate has performed consistently and can be used to drive the adaptive process.

The relative modeling error in the quantity of interest L_4, defined as $L_4(\mathbf{u} - \mathbf{u}^0)/L_4(\mathbf{u})$, is found to be 74.3%. To reduce this error, we adapt the material model as follows. The cell containing the inclusion ω_3 is chosen as an initial guess for the domain of influence Ω_L^0 (with the superscript indicating that this is the initial guess for the domain of influence). Note that this is the cell with the largest error indicator β_k. The local problem (62) is solved on this cell using a well-resolved h-p adaptive mesh, and the enhanced solution $\tilde{\mathbf{u}}$ is constructed. The error in the quantity of interest is reduced and we find $L_4(\mathbf{u} - \tilde{\mathbf{u}})/L_4(\mathbf{u}) = 35.2\%$.

The material model is further adapted by adding neighboring cells to Ω_L^0. The resulting regions and the associated errors are shown in Fig. 10. In each case, we solve a local problem, as described above, and construct the enhanced solution ($\tilde{\mathbf{u}}$). Figure 10 shows that to reduce the modeling error to below 5% (which is considered "engineering tolerance"), it would suffice to stop the adaptive algorithm after computing the enhanced solution ($\tilde{\mathbf{u}}$) on Ω_L^2.

6. SUMMARY AND CONCLUSIONS

The concept of adaptive modeling of materials makes no assumptions about the existence of representative volume elements (RVEs) or the periodicity of microstructure, as is usual in the traditional analysis of composites. Using regularization as part of a larger algorithm, adaptive modeling attempts to deliver material models that satisfy preset accuracy requirements.

In this work, we present a new theory for the *goal-oriented* adaptive modeling of heterogeneous materials and an algorithm for adapting material models based on our theory of local modeling error estimation. Preliminary numerical examples demonstrate the advantages that such modeling techniques have over traditional methods. Extensive numerical experiments, details of a parallel computational infrastructure for the adaptive modeling of heterogeneous materials, incorporation of imaging technology into such analyses, and extensions to nonlinear problems are subjects to be addressed in future work.

ACKNOWLEDGMENTS

We gratefully acknowledge the support of this work by the Office of Naval Research under Grant N00014-95-1-0401 and by the Sandia National Laboratories under Grant BF-2070. Computational resources were provided by the NSF through NPACI, the National Partnership for Advanced Computational Infrastructure, Grant 10152711. Finally, the authors thank Professor Ivo Babuska and Dr. Tarek Zohdi for many useful discussions.

REFERENCES

1. M. Ainsworth and J. T. Oden, A posteriori error estimation in finite element analysis, *Comp. Methods Appl. Mech. Eng.* **142**, 1 (1997).
2. Computational Mechanics Company, Inc., *ProPHLEX User Manual for Version 2.0* (Computation Mechanics Company, Austin, 1996).
3. Z. Hashin, Analysis of composite materials: A survey, *J. Appl. Mech.* **50**, 481 (1983).
4. V. V. Jikov, S. M. Kozlov, and O. A. Oleinik, *Homogenization of Differential Operators and Integral Functionals* (Springer–Verlag, Heidelberg, 1994).

5. J. T. Oden and J. N. Reddy, *An Introduction to the Mathematical Theory of Finite Elements* (Wiley, New York, 1976).
6. J. T. Oden and K. Vemaganti, Adaptive modeling of composite structures: Modeling error estimation, *Int. J. Comp. Civil Str. Eng.* **1**, 1 (2000).
7. J. T. Oden, K. Vemaganti, and N. Moës, Hierarchical modeling of heterogeneous solids, *Comp. Methods Appl. Mech. Eng.* **172**, 3 (1999).
8. J. T. Oden and T. I. Zohdi, Analysis and adaptive modeling of highly heterogeneous elastic structures, *Comp. Methods Appl. Mech. Eng.* **148**, 367 (1997).
9. S. Prudhomme and J. T. Oden, On goal-oriented error estimation for elliptic problems: Application to the control of pointwise errors. *Comp. Methods Appl. Mech. Eng.* **176**, 313 (1999).
10. E. Sanchez-Palencia, Non-homogeneous media and vibration theory, in *Lecture Notes in Physics* (Springer–Verlag, Berlin, 1980).
11. K. Vemaganti and J. T. Oden, Estimation of local modeling error and goal-oriented adaptive modeling of heterogeneous materials. II. A computational environment for adaptive modeling of heterogeneous elastic solids, in preparation.
12. T. I. Zohdi, J. T. Oden, and G. J. Rodin, Hierarchical modeling of heterogeneous bodies, *Comp. Methods Appl. Mech. Eng.* **138**, 273 (1996).